https://doi.org/10.5194/egusphere-2024-1981
Preprint. Discussion started: 25 July 2024

ESD Ideas: Near real-time preliminary detection of carbon dioxide source and sink areas using a Laplacian filter

Yana Savytska[1], Viktor Smolii[2], Nils Weitzel[1]

[1]University of Tübingen, Germany, [2]National University of Life and Environmental Sciences of Ukraine, Ukraine

Correspondence to: Yana Savytska (savytska.yana@mnf.uni-tuebingen.de)

Abstract. The constant rise in atmospheric CO_2 concentrations is warming the planet and causing climate change. Here, we detect ecosystem areas with weighty changes in the CO_2 concentration using digital filtration, similar to image processing techniques, to identify terrestrial CO_2 sources and sinks. This approach may improve CO_2 monitoring capabilities and enable near real-time detection of CO_2 sources and sinks.

Over the past few decades, anthropogenic greenhouse gas (GHG) emissions have led to clearly detectable surface warming (IPCC, 2023). The major part - 75% of all GHGs (Xiao et al., 2016) - is atmospheric carbon dioxide (CO_2). Our research is therefore focused on developing new methods of CO_2 reduction. To facilitate monitoring, reporting and verification, we propose an algorithm for the preliminary detection of CO_2 source and sink areas. This includes the identification of an area as a CO_2 source or sink and it's localization. We test the proposed algorithm using two types of CO_2 data measured at the near-surface layer. We applied digital filtration (Burger and Burge, 2016) to a CO_2 concentration (CDC) dataset to detect sink and source areas and CO_2 flux data to verify the results. Identifying the type of area as a CO_2 sink or source could help to improve the usability and functionality of CO_2 monitoring services, e.g. the Copernicus Atmosphere Monitoring Service, the NASA Carbon Monitoring System, or to assess the role and efficiency of different ecosystems in the global carbon cycle.

The response of an ecosystem to external and internal disturbances is reflected in the carbon balance (CB) of its sources and sinks (Xiao et al., 2016). Recent studies have described ecosystem responses to disturbances using functional indices – NDVI (Liu et al., 2022), NPP, GPP (Mahecha et al., 2022), SIF (Li et al., 2022), biodiversity (Mahecha et al., 2022) and others in the complex multivariate models (Holm et al., 2023). This makes them potentially accurate but also more resource intensive, less straightforward and less sensitive to short-term changes. Therefore, we propose the CDC as an integral parameter for the near real-time detection of CO_2 sources and sinks that can also be applied to long-term observations.

Existing CO_2 monitoring services provide spatially distributed CDC on a global scale (Weir and Ott, 2022; CAMS, 2020). This does not include the detection of local CO_2 sink and source areas. A possible solution could be an edge detection using digital filtration. This could sharpen the boundaries and make it possible to detect the CO_2 sink and source areas with a size corresponding to the resolution of the CDC dataset. Digital filtration is a well-known tool also used in Geosciences, for example, to detect plumes of burning biomass (Goudar et al., 2023). Before applying digital filtration, we need to consider the size of the areas, the characteristics of the internal physical, chemical and biological processes, and the CB of each area. We work with the concept of a "small area" as a cell whose size depends on the inertia rate of chemical and physical

https://doi.org/10.5194/egusphere-2024-1981
Preprint. Discussion started: 25 July 2024

processes, and interpret it as a closed ecosystem based on the characteristics described below. Here the term "small area" is an analogue of "small ecosystem", defined by a set of characteristics and their values that describe an ecosystem in all its parts with a slight (or within the specified range) deviation. This deviation can be neglected at any time and any place within the ecosystem.

The carbon balance can be seen as a strictly hierarchical system in which lower level subsystems separately describe the CB in terms of its environmental and other conditions. The components of the subsystems are spatially distributed, defining the unique set of components of each area and determining the variability of environmental characteristics in different areas. To identify fluxes in the upper atmospheric CB, we use two principles. The first is the direction of CO_2 flows (suffixes "In" and "Src" into the atmosphere or "Out" and "Sink" - out of it). The second principle is relative to the boundary of the area - the prefix "Env" for the external environment and "Int" for internal processes and objects. Accordingly, we describe the total CB of the area of interest by Eq. (1):

$$CB = EnvIn - EnvOut + \sum IntSrc_k - \sum IntSink_i \quad (1)$$

where $EnvIn$ – the flux intensity of the CO_2 injection from the external environment, $EnvOut$ – the flux intensity of the CO_2 emission to the external environment, $\sum IntSrc_k$ – the total flux intensity of internal CO_2 sources, $\sum IntSink_i$ – the total flux intensity of internal CO_2 sinks.

The external components of CB and their effects are independent of the characteristics of the area of interest, unlike the internal components. The internal components of the CB clearly correspond to the components of the ecosystem - plants of certain species, soil, etc. This balance defines the total amount of CO_2 in the atmosphere of the area and consequently the *CDC=Func(CB)*.

The process of gas injection is inertial. For example, CO_2 emissions from a power plant do not change the CDC in every part of the Earth's atmosphere, they only affect the neighbouring areas, and even then, it happens slowly, over some time. This process is described by diffusion and environmental conditions. We assume that the CDC in a "small area" that was formed at some earlier time does not change significantly during the time it takes the satellite to measure the CDC in neighbouring "small areas", and interpret a data acquisition as a "monochrome image snapshot" of data.

The next two characteristics are also relevant to the definition of "small area". Firstly, the characteristics of physical and chemical inertness in the atmosphere and soils will lead to different spatial distributions of the characteristics, and the speed of these processes will affect the size of the cells by considering the value limit of the specified deviation. Secondly, in digital filtration, the size of the cells processed must be the same, which is limited by the size of the smallest area of the system. Another filtration requirement concerns the presence and location of neighbouring areas around the area of interest. According to the mathematical rules of sliding filtration (Aubry et al., 2014), cells should be located close to each other and partially have common boundaries, as shown in Fig. 1a. This requirement also leads to the neglect of air mass transport, as the short distances between the area of interest and neighbouring areas minimize its impact – transferred external air masses

https://doi.org/10.5194/egusphere-2024-1981
Preprint. Discussion started: 25 July 2024

will give approximately the same $EnvIn$ and $EnvOut$ components in all neighbouring areas (in the filter focus). The small size and close location of cells also make it possible to detect the influence of external factors with synchronous changes in the monitored parameter with equal or proportional values (Fig. 1b).

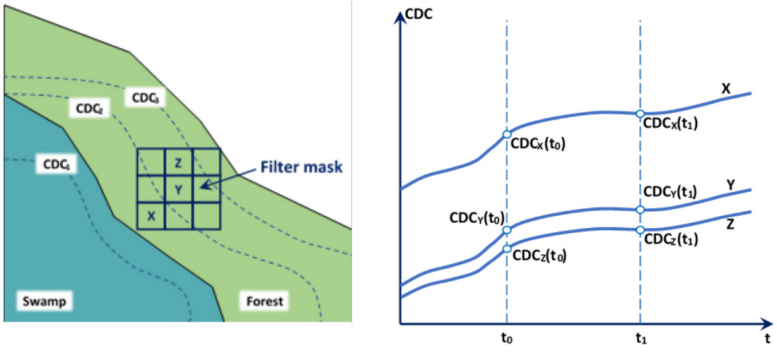

(a) An example of CO_2 source and sink location (b) An example of synchronous CDC changes over time

Figure 1: Spatial and temporal CDC changes.

For example, at time t_0, we expect different concentrations at points *X, Y* and *Z* – $CDC_X(t_0)$, $CDC_Y(t_0)$ and $CDC_Z(t_0)$ accordingly. Concerning the distance from the swamp (CO_2 source) and how deep each point is located in the forest (CO_2 sink), we assume that concentrations are related according to inequality (2).

$$CDC_X(t_1) > CDC_X(t_0), CDC_Y(t_1) > CDC_Y(t_0), CDC_Z(t_1) > CDC_Z(t_0) \quad (2)$$

If, at time point $t_1 > t_0$, the concentrations change according to the relationship (2), while all internal environmental conditions remain stable, this will result in a simultaneous multi-point (*X-Z*) increase in CDC, as shown in (3,4).

$$CDC_X(t_1) > CDC_X(t_0), CDC_Y(t_1) > CDC_Y(t_0), CDC_Z(t_1) > CDC_Z(t_0) \quad (3)$$

$$\Delta CDC_X \simeq \Delta CDC_Y \simeq \Delta CDC_Z, \text{ where } \Delta CDC_{XYZ} = CDC_{XYZ}(t_1) - CDC_{XYZ}(t_0) \quad (4)$$

Relationships 1-3 describe the connectivity and synchronicity of concentration change processes, but not their randomness. For example, equation (5) describes a synchronous increase in concentration due to daytime solar radiation, based on the conditions outlined in (4).

$$CDC_X(t_0) < CDC_X(t_1), CDC_Y(t_0) < CDC_Y(t_1), CDC_Z(t_0) < CDC_Z(t_1) \quad (5)$$

The above relationships and assumptions lead us to the conclusion that the CO_2 deltas shown in Eq. (4) correspond to the synchronous CDC changes for the whole area under the influence of external environmental conditions.

Based on Eq. (1), the difference between the CBs for two small neighbouring ecosystems can be described by Eq. (6):

https://doi.org/10.5194/egusphere-2024-1981
Preprint. Discussion started: 25 July 2024

$$CB_1 - CB_2 = (EnvIn_1 - EnvOut_1 + \sum IntSrc_{k1} - \sum IntSink_{i1}) - (EnvIn_2 - EnvOut_2 + \sum IntSrc_{k2} - \sum IntSink_{i2}) \quad (6)$$

According to the concept of small neighbouring areas, the values of EnvIn and EnvOut are equal in all cells, therefore the result of (6) can be interpreted as the difference in CO_2 fixation efficiency with (7):

$$CB_1 - CB_2 = (\sum IntSrc_{k1} - \sum IntSink_{i1}) - (\sum IntSrc_{k2} - \sum IntSink_{i2}) \quad (7)$$

If the characteristics of the neighbouring ecosystems are similar (each of the $IntSrc_{k1}$ sources of the first area is equal to $IntSrc_{k2}$ in the second neighbouring area, and each of the $IntSink_{i1}$ is equal to $IntSink_{i2}$), then based on (6) it is possible to identify the emergence of the external CO_2 source according to (8):

$$CB_1 - CB_2 = (EnvIn_1 - EnvOut_1) - (EnvIn_2 - EnvOut_2) \quad (8)$$

Each ecosystem is surrounded by neighbouring ecosystems, which can be represented in the Cartesian coordinate system with a set of indices in the vertical, horizontal and diagonal directions:

$$\begin{vmatrix} 4 & 3 & 2 \\ 5 & 0 & 1 \\ 6 & 7 & 8 \end{vmatrix} \quad (9)$$

When we form the convolutional filter of the difference between the central element and a given element, the coefficient "1" is placed in the centre of the matrix (zero index) and the coefficient "-1" is in the position defined by a given index. Using this indexing system and the convolutional filter principle, the difference (6) can be described in a matrix operation form over CB data as:

$$F(CB) = (CB_1 - CB_2) \Rightarrow (1 \times CB_1 + (-1) \times CB_2) \Rightarrow \begin{vmatrix} 0 & 0 & -1 \\ 0 & 0 & 1 \\ 0 & 0 & 0 \end{vmatrix} \quad (10)$$

The central index corresponds to the area of interest, and the rest are neighbouring areas. The matrix for evaluating the difference between all 8 neighbouring cells is as follows:

$$F(CB) = \sum_{i=1}^{i=8}(CB_0 - CB_i) \Rightarrow F(CB) = \begin{vmatrix} -1 & -1 & -1 \\ -1 & 8 & -1 \\ -1 & -1 & -1 \end{vmatrix} \quad (11)$$

The area of interest is identified as a CO_2 sink or source based on its CDC in relation to that of the neighbouring areas. This means that the resolution of the dataset and the number of neighbouring areas define the area of identification. Depending on the expected sizes of CO_2 sinks and sources, the resolution of the dataset and the size of the matrix of coefficients can be adjusted. This option shows the universality of the proposed algorithm with respect to the sizes of CO_2 sources and sinks.

This matrix corresponds to the Laplacian convolutional filter. This is a second order filter used for edge detection and feature extraction (Aubry et al., 2014). Unlike first-order filters, we do not need separate filters to detect and then combine vertical and horizontal edges, as the Laplacian filter detects all edges regardless of direction.

https://doi.org/10.5194/egusphere-2024-1981
Preprint. Discussion started: 25 July 2024

In order to apply the Laplacian filter to a CDC dataset formed by carbon balances, we performed a convolution operation, which mathematically means a combination of two matrices, in our case one containing the CDCs and the other – the filter coefficients. The convolution operation, represented by Eq. (12), involves sliding the filter over the dataset, multiplying the CDCs by the corresponding coefficients and adding them up. The result is a new dataset of the same size as the original, but the calculated CDC differences can be positive, negative or zero. A positive value after digital filtration means that the original CDC in the area of interest is greater than the average CDC in the neighbouring areas. This area is identified as containing the CO_2 source. Conversely, an area with a negative value is identified as containing a CO_2 sink. A zero value indicates CO_2 homogeneous areas.

$$CDC_{filtered} = \begin{bmatrix} CDC_4 & CDC_3 & CDC_2 \\ CDC_5 & CDC_0 & CDC_1 \\ CDC_6 & CDC_7 & CDC_8 \end{bmatrix} \times \begin{bmatrix} -1 & -1 & -1 \\ -1 & 8 & -1 \\ -1 & -1 & -1 \end{bmatrix} \quad (12)$$

This filter, with a size of 3x3 cells, covers the area of 4.8x6.6 km when scanned with OCO satellites (OCO, 2015). It is optimal for our task in terms of processing time and computational complexity – 15 arithmetic operations for an area of interest, and does not require additional computational resources. This partially provides real-time computation for the 6 areas in the satellite scan area strip, which requires 90 operations per second.

The test results of the proposed algorithm (Appendix A) for CO_2 source and sink area detection show that it is sufficient for a rapid fire response or for a detailed subsequent study of the CO_2 fixation characteristics of the vegetation in the sink area. We do not consider CO_2 advection for the source area detection because the influence of air mass transport is small. It is close to 6% at a wind speed of 30 m/sec and a scanning time of 3 data rows by satellite for 1 second (OCO, 2015). This value is applicable for the tasks of rough CO_2 source and sink areas detection.

Appendix A: Results of CO_2 source and sink areas detection with Laplacian filter

To test the proposed algorithm with a CO_2 source area detection, we chose a large fire event in the Serengeti National Park, Tanzania, which started on 22 July 2016 and lasted for 31 days. We used CDC values as an indicator of a fire area and CDC spatial differences to detect area boundaries. For the experiment, we took the CDCs for 27 July 2016 (Weir and Ott, 2022), the fifth day after the fire had started, to avoid the influence of additional CO_2 from a previous fire event in the area. The CDC distribution for this date is shown in Fig. A1a, but it is not possible to see the clear boundaries of the area, because the spatial CDC differences are blurred. In order to detect the fire area boundaries, we applied the Laplacian filter, assuming that all the CDCs in the area were measured at the same time. The results are shown in Fig. A1b, where each cell has a different shading, representing a change in CDC intensity. The dark shaded cells are defined as CO_2 sources.

To verify the obtained results, we compared them with a CO_2 flux for the above-ground layer, taken from an available CO_2 flux dataset (Lesley, 2020). The flux data are presented in Fig.A2a with isolines showing the rate of CDC changes. The greater the number of isolines around the point, the faster the concentration changed. The comparison of the experimental

https://doi.org/10.5194/egusphere-2024-1981
Preprint. Discussion started: 25 July 2024

results and the flux data showed a rough agreement in the detection of the CO_2 source area. The differences in location can be explained by the higher spatial resolution of the flux data. However, the process of obtaining flux data requires either, a complex information model that is not real-time, or that a satellite to fly over the same point on Earth at least twice. In situations that require a more operational response, such as the start of a large forest fire near a populated area or an emergency at a power plant with high CO_2 emissions, this may be too long. In our experiment, we chose available CDC data, interpreted as "at the moment", and applied a Laplacian filter to detect CO_2 source areas. In reality, the proposed method can be applied to the satellite scanned data "strip" in real time.

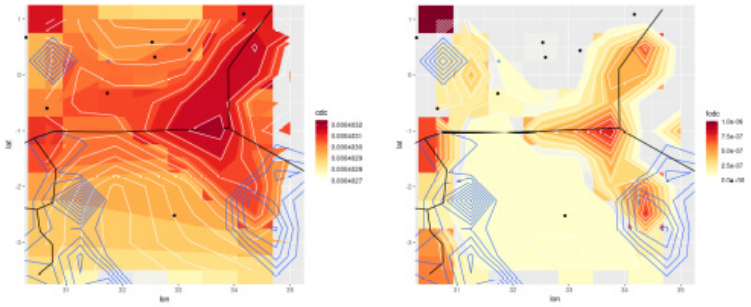

(a) CDC distribution in the fire place area (a) The obtained results and their verification

Figure A1: A spatial CDC distribution in the area of the fireplace and its boundaries detection with the proposed method.

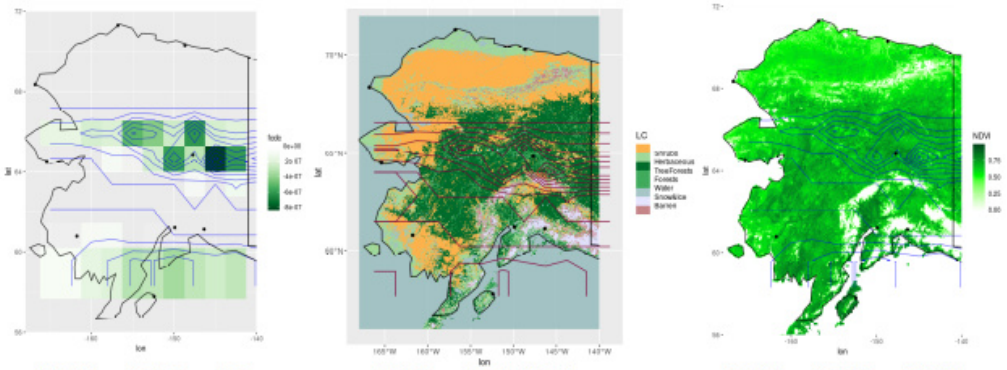

(a) Filtered CDC spatial distribution (b) LC spatial distribution (c) Filtered CO2 and NDVI distribution

Figure A2: Verification of the CO_2 sink detected area with vegetation indices.

Identifying areas that are CO_2 sinks is different from identifying areas that are short-term sources of CO_2. The most important terrestrial CO_2 sink is vegetation, the characteristics of which depend mainly on the time of day and the season.

https://doi.org/10.5194/egusphere-2024-1981
Preprint. Discussion started: 25 July 2024

The size of large forests does not change over hours or days, but over years or decades. We therefore need to define the boundaries of large forests once and then monitor them.

For our experiment, we chose CDC data (CAMS, 2020) for the period of active vegetation growth and analyzed data for Alaska in June 2016. We considered land cover (LC) type, biomass and growth phase (NDVI) as parameters of CO_2 fixation. First, we compared the CDC data processed with the Laplacian filter (Fig. A2a) with the LC types in Alaska. The results of this comparison are shown in Fig. A2b, where the LC data are presented in the FAO Land Cover Classification System (LCSS) (Friedl and Sulla-Menashe, 2019). The isolines in the figure show the change in CDC intensity, which roughly correspond to the formal boundaries of the LCCS vegetation classes. Forests with more than 60% tree cover (Di Gregorio, 2005): evergreen forests, deciduous forests and mixed forests show a higher CO_2 fixation.

In contrast, there is little spatial difference in CO_2 fixation between the areas covered by shrubs and herbs in Fig. A2b, possibly due to the small amount of biomass in these ecosystems and the potential influence of the nearby ocean.

The filtered CDC is nearly negligible on the mountain tops due to the uniform barren ground, ice, and snow zones. The NDVI (Fig. A2c) is also less significant in these areas. In contrast, the central part of Alaska which is covered by a large amount of evergreen biomass with high NDVI is identified as a CO_2 sink. Mountains protect this area from the influence of the oceans. These results could help in further work to explain the different CO_2 fixation potential in different subregions of these areas based on the absolute values of processed CDCs.

Data availability

Data are available from https://doi.org/10.5281/zenodo.12532657.

Author contributions

YS conceptualised the study and designed the methodology; YS and VS processed the data; YS wrote the manuscript; VS and NW reviewed and partly edited the manuscript.

Competing interests

The contact author has declared that none of the authors has any competing interests.

Acknowledgements

This research was carried out in the SPACY group at the University of Tübingen (Germany), as part of "Research@Tübingen" fellowship and an individual project of the first co-author within the Philipp Schwartz scholarship program. Yana Savytska also acknowledges support from Prof. Dr. Kira Rehfeld, SPACY group leader.

https://doi.org/10.5194/egusphere-2024-1981
Preprint. Discussion started: 25 July 2024

References

Aubry, M., Paris, S., Hasinoff, S. W., Kautz, J. and Durand, F., Fast Local Laplacian Filters: Theory and Applications. ACM Trans. Graph. 33, 5, Article 167, 14 pages. https://doi.org/10.1145/2629645, 2014.

Burger W., Burge M. J. Digital Image Processing: An Algorithmic Introduction. Digital Image Processing, 2nd edition, Springer Nature, London, XXIII, 811 p., https://doi.org/10.1007/978-1-4471-6684-9, 2016.

CAMS global inversion-optimised greenhouse gas fluxes and concentrations, https://ads.atmosphere.copernicus.eu/cdsapp#!/dataset/cams-global-greenhouse-gas-inversion?tab=overview [data set], 2020, last access: 01 May 2024.

Friedl, M., Sulla-Menashe, D. MCD12Q1 MODIS/Terra+Aqua Land Cover Type Yearly L3 Global 500m SIN Grid V006 [data set]. NASA EOSDIS Land Processes Distributed Active Archive Center, https://doi.org/10.5067/MODIS/MCD12Q1.006, 2019.

Goudar, M., Anema, J. C. S., Kumar, R., Borsdorff, T., and Landgraf, J.: Plume detection and emission estimate for biomass burning plumes from TROPOMI carbon monoxide observations using APE v1.1, Geosci. Model Dev., 16, 4835–4852, https://doi.org/10.5194/gmd-16-4835-2023, 2023.

Di Gregorio, A. Land cover classification system: classification concepts and user manual: LCCS. Number 8. Food & Agriculture Organization, Rome, Italy. ISBN 92-5-104216-0, https://www.fao.org/4/x0596e/x0596e00.htm, (last access: 01 May 2024), 2005.

Holm, J. A. et. al. Exploring the impacts of unprecedented climate extremes on forest ecosystems: hypotheses to guide modeling and experimental studies, Biogeosciences, 20, 2117–2142, https://doi.org/10.5194/bg-20-2117-2023, 2023.

IPCC, 2023: Summary for Policymakers. In: Climate Change 2023: Synthesis Report. Contribution of Working Groups I, II and III to the Sixth Assessment Report of the Intergovernmental Panel on Climate Change [Core Writing Team, H. Lee and J. Romero (eds.)]. IPCC, Geneva, Switzerland, pp. 1-34, https://doi.org/10.59327/IPCC/AR6-9789291691647.001, 2023.

Ott, L., GEOS-Carb CASA-GFED Daily Fire and Fuel Emissions 0.5 degree x 0.5 degree V2, Greenbelt, MD, USA, Goddard Earth Sciences Data and Information Services Center (GES DISC) [data set], https://doi.org/10.5067/IYZIZJ8ZFZHU, 2020.

https://doi.org/10.5194/egusphere-2024-1981
Preprint. Discussion started: 25 July 2024

Li C, Peng L, Zhou M, Wei Y, Liu L, Li L, Liu Y, Dou T, Chen J, Wu X. SIF-Based GPP Is a Useful Index for Assessing Impacts of Drought on Vegetation: An Example of a Mega-Drought in Yunnan Province, China. *Remote Sensing*. 14(6):1509, https://doi.org/10.3390/rs14061509, 2022.

Liu, L., Jiang, Y., Gao, J., Feng, A., Jiao, K., Wu, S., Zuo, L., Li, Y., Yan, R. Concurrent Climate Extremes and Impacts on Ecosystems in Southwest China. Remote Sens., 14, 1678, https://doi.org/10.3390/rs14071678, 2022.

Mahecha, M. D., Bastos, A., Bohn, F. J., Eisenhauer, N., Feilhauer, H., Hartmann, H., Hickler, T., Migliavacca, M., Otto, F. E., Peng, J., Quaas, J., Tegen, I., Weigelt, A., Wendisch, M., & Wirth, C. Biodiversity loss and climate extremes - Study the feedbacks. Nature, 612(7938), 30-32, https://doi.org/10.1038/d41586-022-04152-y, 2022.

Orbiting Carbon Observatory (OCO) Algorithm Theoretical Basis Document (ATBD) https://docserver.gesdisc.eosdis.nasa.gov/public/project/OCO/OCO_L2_ATBD.pdf, 2015, last access: 01 May 2024.

Xiao, J., Liu, S., and Stoy, P. C.: Preface: Impacts of extreme climate events and disturbances on carbon dynamics, Biogeosciences, 13, 3665–3675, https://doi.org/10.5194/bg-13-3665-2016, 2016.

Weir, B., Ott, L., and OCO-2 Science Team, OCO-2 GEOS Level 3 daily, 0.5x0.625 assimilated CO_2 V10r, Greenbelt, MD, USA, Goddard Earth Sciences Data and Information Services Center (GES DISC) [data set], https://doi.org/10.5067/Y9M4NM9MPCGH, 2022.